Dynamic Performance of C80 Railway Wagon Under the Influence of Wheel Polygons and Typical Mode Shapes of the Car Body

Yuru Li[1,2] ✉ – Gangjian Zhou[2] – Xiangwei Li[1] – Tao Zhu[3] – Shangchao Zhao[1] – Chunlei Zhao[1] – Junke Xie[2] – Shoune Xiao[3]

[1] CRRC Qiqihar Rolling Stock Co., Ltd., China
[2] Henan University of Science and Technology, College of Vehicle and Traffic Engineering, China
[3] Southwest Jiaotong University, State Key Laboratory of Rail Transit Vehicle System, China

✉ lyr@haust.edu.cn

Abstract *To investigate the influence of typical mode shapes and wheel polygons on the dynamic characteristics of railway freight car body, this study takes railway freight wagon C80 as the research object. Vehicle-level and system-level finite element models of the C80 railway wagon were developed, revealing that the lateral and vertical stiffness of railway freight cars significantly affects system mode. Furthermore, co-simulation using NASTRAN and SIMPACK was used to establish a fully flexible dynamic model of the C80 wagon. The influence of typical modal frequencies on the dynamic performance of the wagon was analyzed considering the wheel polygon and wear parameters. The results show that suppressing the torsional mode shape of the railway wagon reduces its impact on the derailment coefficient, wheel load reduction rate, axle transverse force and overturning coefficient by over 40 %. When the train speed corresponds to the polygon order, the wheel load reduction rate increases with the polygon wear depth under both the 10th order and 18th order conditions, by as much as 14.4 % when wear depth increases from 0.01 mm to the 0.05 mm for the 18th order condition. In addition, under the 6th order, 10th order, 16th order and 18th order polygon conditions, suppressing the torsional mode notably increased the wheel load reduction rate, especially under the 6th order polygon condition. This research provides valuable guidance for optimizing suspension parameters and controlling polygonal wear in railway wagons, offering a guiding basis for enhancing their dynamic performance of railway wagons.*

Keywords *full flexibility, C80 railway wagon, dynamic models, wheel polygons suspension parameters*

Highlights
- *Built first fully flexible C80 wagon model via Nastran–Ansys co-simulation.*
- *FE results show lateral/vertical stiffness strongly affects wagon system modes.*
- *Findings guide suspension design and help control wear, boosting dynamic performance.*

1 INTRODUCTION

The polygonization of railway wagon wheels (the periodic non-roundness of the wheelset) aggravates the impact of wheels and rails, resulting in increased vibration, noise, and fatigue damage of components, and even posing potential safety risks. At the same time, the suspension parameters of the running part, including spring rate, damping coefficient and positioning stiffness, directly affect the running smoothness of railway wagons, curving abilities, and wheel-rail interaction. Therefore, it is necessary to conduct a systematic study on the combined influence of wheel polygonization and suspension parameters on dynamic performance of railway wagons.

The polygonal wear of railway vehicles is essentially a periodic irregularity resulting from uneven circumference wear, typically with an order number between 1 and 30, and a wave depth of approximately 1 mm [1]. This phenomenon excites the bogie through wheel-rail contact, reduces the fatigue life of components, and deteriorates the dynamic performance of the train [2]. Therefore, the polygon wear of the wheels has become a persistent long-term issue in railway operation. Extensive research—both experimental and theoretical—has been conducted to investigate the formation mechanisms and dynamic effects of wheel polygonization. Li et al. [3] systematically analyzed its impact on the running stability of the vehicle through field measurement and numerical simulation, revealing that for polygon orders of 1 to 10 with a wave depth of 0.2 mm, the critical speed drops to just 61 km/h, significantly affecting stability. Tao et al. [4] and Cai et al. [5] studied the 6th to 8th order polygon wear in metro vehicles traveling at 70 km/h and identified the wheel-rail P2 force as the root cause of polygon formation. Yang et al. [6] used the rigid-flexible coupling model. They found that considering wheelset and track elasticity and applying multi-cut re-profiling technology effectively reduces flange polygon wear in heavy-haul trains. Recently, Jin et al. [7] highlighted the emergence of high-order wheel polygons, whose associated high-frequency vibrations accelerate fatigue damage in bogies and track components. Zhou et al. [8] proposed that the 4th order bending resonance of the wheelset was the main reason for the 20th order polygon wear, considering the non-Hertz contact and track irregularities. Johansson and Nielsen [9] as well as Johansson and Andersson [10] identified the vertical anti-resonance of the track at 165 Hz as the main reason in the growth of 14th to 20th order polygon wheel roughness. Similarly, Ye et al [11] and Yang et al. [12] showed through modal and dynamic simulation analyses that the rail B3 mode induces resonance in the wheel-rail system, driving the high-order polygonization. Wu et al. [13] confirmed experimentally that the coupling resonance of the framework plays a key role in the forming higher-order polygons.

Additional studies linked polygonal wear to fatigue damage in vehicle components. Fu et al. [14] identified low-frequency wheel-rail impacts as the cause of fatigue cracks in the bogie frame. Wang et al. [15] found that the rail corrugations combined with wheel polygons was the main contributor of fatigue damage of the bogie

DOI: 10.5545/sv-jme.2025.1462

frame. Liu et al. [16], Song et al. [17] and Wu et al. [18] using rigid-flexible coupling dynamics models, demonstrated the wheel polygons produce large fluctuations in wheel-rail interaction forces, where short-wavelength components excite high-frequency vibrations in rails and sleepers. Barke et al. [19] analyzed in detail their adverse on both vehicle components and track systems. Zhang et al. [20] found that high-order wheel polygons with the equivalent roughness generate stronger wheel-rail noise and internal noise, reducing passenger comfort.

The suspension system of railway vehicle, comprising primary and secondary suspension, also plays a crucial role in dynamic properties of vehicles. Thomas et al. [21] studied and verified the effects of suspension, curve settings, and track defects on vehicle traverse and roll angle. Park et al. [22] studied the effects of suspension system, wheel-rail creep coefficient, and track excitation on vehicle lateral stability. Based on the rigid-flexible coupling dynamic model considering the flexibility of the frame, Ma et al. [23] considered frame flexibility and demonstrated that non-diagonal spring stiffness greatly affects curve-passing speed. Guan et al. [24] found that reducing wheelset mass and inertia while increasing suspension stiffness and damping improves the critical speed of the hunting motion. Xiao et al. [25] used UM software to analyze CRH2 EMU dynamics and found that the vertical and lateral stiffness of the primary springs and damping of the secondary transverse shock absorbers dominate the vibration response. Lei et al. [26] used SIMPACK to assess a subway vehicle performance, showing that the influence of a series of suspension longitudinal and lateral stiffness on the nonlinear critical velocity first increases and then decreases. Mousavi Bideleh et al. [27] emphasizes that optimized suspension parameters can effectively reduce wheel and rail wear and enhance driving safety.

To broaden the scope of the literature review and strengthen the scientific context, it is essential to include research addressing the structural behavior and optimization of railway vehicles based on their dynamic behavior, particularly focusing on bogie frames and car bodies, which share many dynamic interaction aspects with the C80 freight wagon analyzed in this study. As the primary interface between vehicle and track, the railway bogie plays a critical role in transmitting and distributing loads arising from track irregularities and operational dynamics. Several studies have investigated bogie frame design through structural and topological optimization combined with dynamic analysis, highlighting that geometry, stiffness distribution, and material selection substantially influence fatigue life, vibration response, and stability [28-31]. The car body, as the primary load-bearing structure of the railway vehicle, has been extensively studied not only in terms of its mechanical strength but also to its dynamic behavior, which plays a fundamental role in the overall performance and safety of freight wagons. Recent research emphasizes that the natural mode shapes of the car body, particularly lateral, vertical, and torsional vibrations, significantly influence key dynamic parameters such as derailment coefficients, axle forces, and wheel wear. In particular, investigations on the C80 freight car revealed that specific modal frequencies, together with wheel polygonal wear, can markedly affect the vehicle's dynamic response.

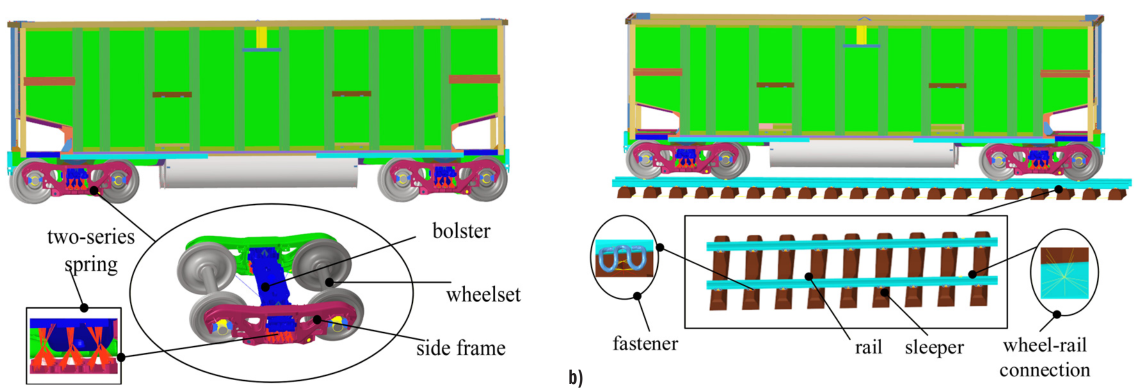

Fig. 1. Construction of the finite element model of the C80 railway wagon; a) vehicle-level C80 railway freight car, and b) system-level C80 railway freight car

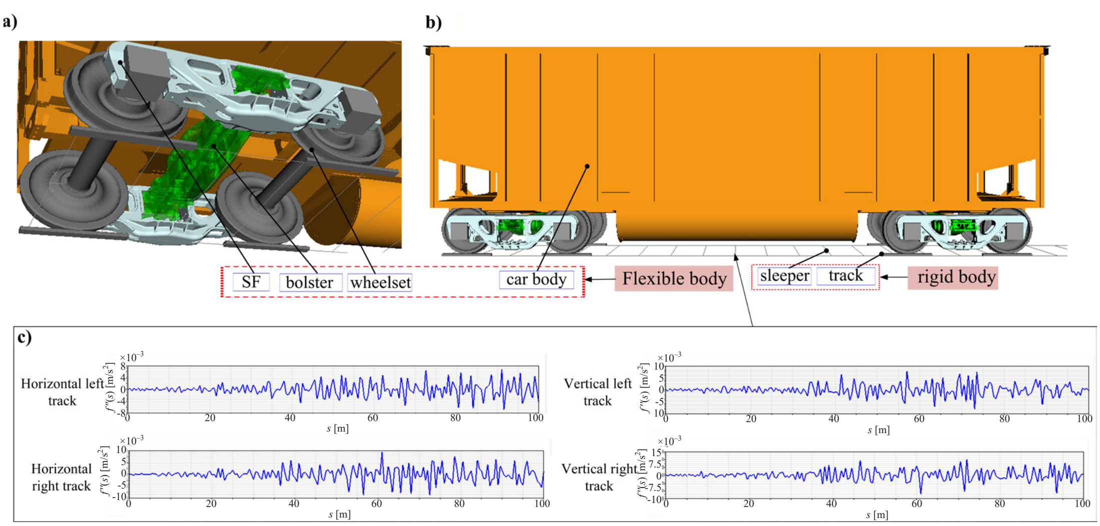

Fig. 2. A fully flexible model of the C80 railway wagon; a) partial enlarged view of the running section, b) fully flexible model of the C80railway wagon, and c) orbital spectral excitation

Through detailed finite element modeling and advanced co-simulation methods, these studies demonstrate that controlling or suppressing certain torsional mode shapes can lead to substantial improvements in dynamic stability and reductions in critical dynamic loads. Within this context, incorporating the dynamic modal characteristics of the car body into structural design provide a valuable perspective, as it offers an important complement to traditional approaches focused primarily on structural optimization and weight reduction, ultimately contributing directly to safer and more efficient freight vehicle designs [32-35]. Comparative analyses between conventional and modern lightweight materials show that tailored material-structure combination can achieve an optimal balance between mass reduction and dynamic performance, offering insights directly applicable to freight wagon design. Zhou et al. [36] and Yu et al. [37] studied the vibration responses of railway vehicles and provided an effective reference for the preliminary design of secondary suspension of railway vehicles.

The above studies show that wheel polygonization, together with the parameters of the first-series and two-series suspension, have an important impact on the dynamic performance of the vehicle system. However, research specifically addressing the interaction between first-series suspension parameters and typical modes in the dynamic performance of railway wagons remains insufficient and requires further investigation. In this paper, the modal characteristics of the C80 wagon are analyzed by developing both vehicle-level and system-level finite element models. The effects of first-series and second-series suspension parameters on the modal frequencies are examined, and the corresponding typical mode shapes most relevant to dynamic behavior are identified.

2 METHODS

Taking the C80 railway wagon as the research object, which consists of four primary components: the car body, side frame, rocker and wheelset, as shown in Fig. 1, vehicle-level and system-level C80 railway wagon finite element models are established using finite element software.

Firstly, finite element models of the car body, bolster, and side frame (SF) were established in NASTRAN, and both BDF and OP2 files were generated. These files were then imported into SIMPACK to generate the FBI file containing the modal and stiffness information. Based on this data, a dynamic model of the railway wagon was established in SIMPACK. The flexible car body, bolster, wheelset, and side frame were subsequently imported to replace the rigid counterparts, resulting in a fully flexible dynamic model of the railway wagon on a rigid track, as shown in Fig. 2b. Figure 2a presents a partially enlarged view of the running section of the C80 railway wagon, while Fig. 2c shows the orbital spectral excitation used in simulation. The vehicle model assumes a fixed wheelbase of 8.2 m, an axle load of 25 t, and a total load of 80 t.

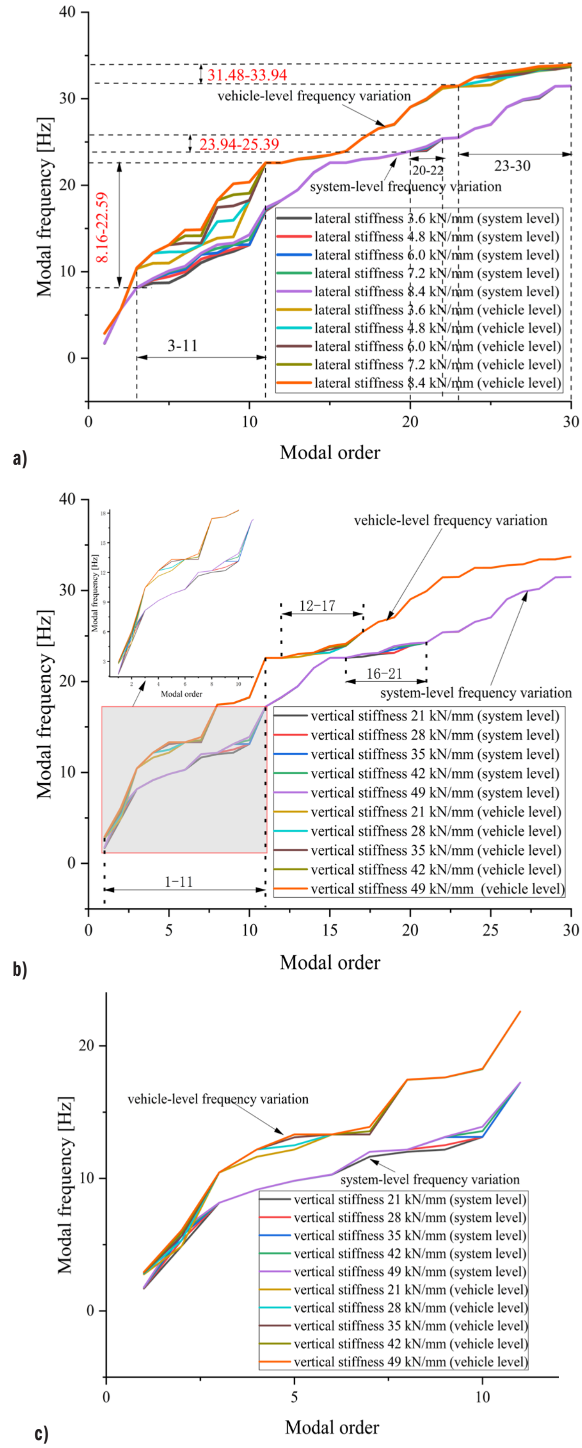

Fig. 3. Variation of mode attitude frequency under different: a) transverse stiffnesses, b) vertical stiffnesses, and c) local diagram of vertical stiffness

3 RESULTS AND DISCUSSION

3.1 Influence of a Series of Lateral and Vertical Stiffness

To analyze the influence of first-series lateral and vertical stiffnesses on the system modal frequency, parametric variations were introduced based on the original lateral stiffness of 6 kN/mm and vertical stiffness of 35 kN/mm. A variation range of ±40 % was applied. Accordingly, the lateral stiffness was set to 3.6 kN/mm, 4.8 kN/mm, 7.2 kN/mm, and 8.4 kN/mm, while the vertical stiffness was varied to 21 kN/mm, 28 kN/mm, 42 kN/mm, and 49 kN/mm. For each stiffness configuration, the first 30 modal frequencies were obtained through vehicle-level, system, and finite element calculations and were compared with the modal frequencies of the initial lateral and vertical stiffness. The comparison results are shown in Fig. 3.

As shown in Fig. 3a, both the vehicle-level and the system-level modal frequency increase with the rise in lateral stiffness, particularly in the 3rd to 11th order, where the changes are the most pronounced. At higher modal orders, the system-level frequencies show noticeable variation only in the 20th to 22nd order, while the vehicle-level modal frequency exhibit changes mainly in the 23rd to 30th modes. In these ranges, the modal frequencies increase respectively from 8.16 Hz to

22.59 Hz, 23.94 Hz to 25.39 Hz, and 31.48 Hz to 33.94 Hz, indicating that the modal frequencies within these three segment ranges are highly sensitive to changes in lateral stiffness. Similarly, Fig. 3b shows that both vehicle-level and system-level modal frequencies increase with vertical stiffness in the 1st to 11th order range, and the modal frequency rise from 1.79 Hz to 17.22 Hz. Sensitivity to vertical stiffness also appears in the mid-order modes: the 12th to 17th vehicle level modes and the 16th to 21st modal frequencies increase from 22.59 Hz to 25.39 Hz and from 22.6 Hz to 24.28 Hz, respectively. This indicates that modal frequencies in these three-segment range are strongly sensitive to changes in vertical stiffness. Overall, the first series of lateral and vertical stiffness have a significant influence on the modal frequency of the system, and thus the modal frequencies associated with the typical vibration modes of both the railway wagon and the railway freight car can be effectively adjusted by changing the suspension parameters of the first series.

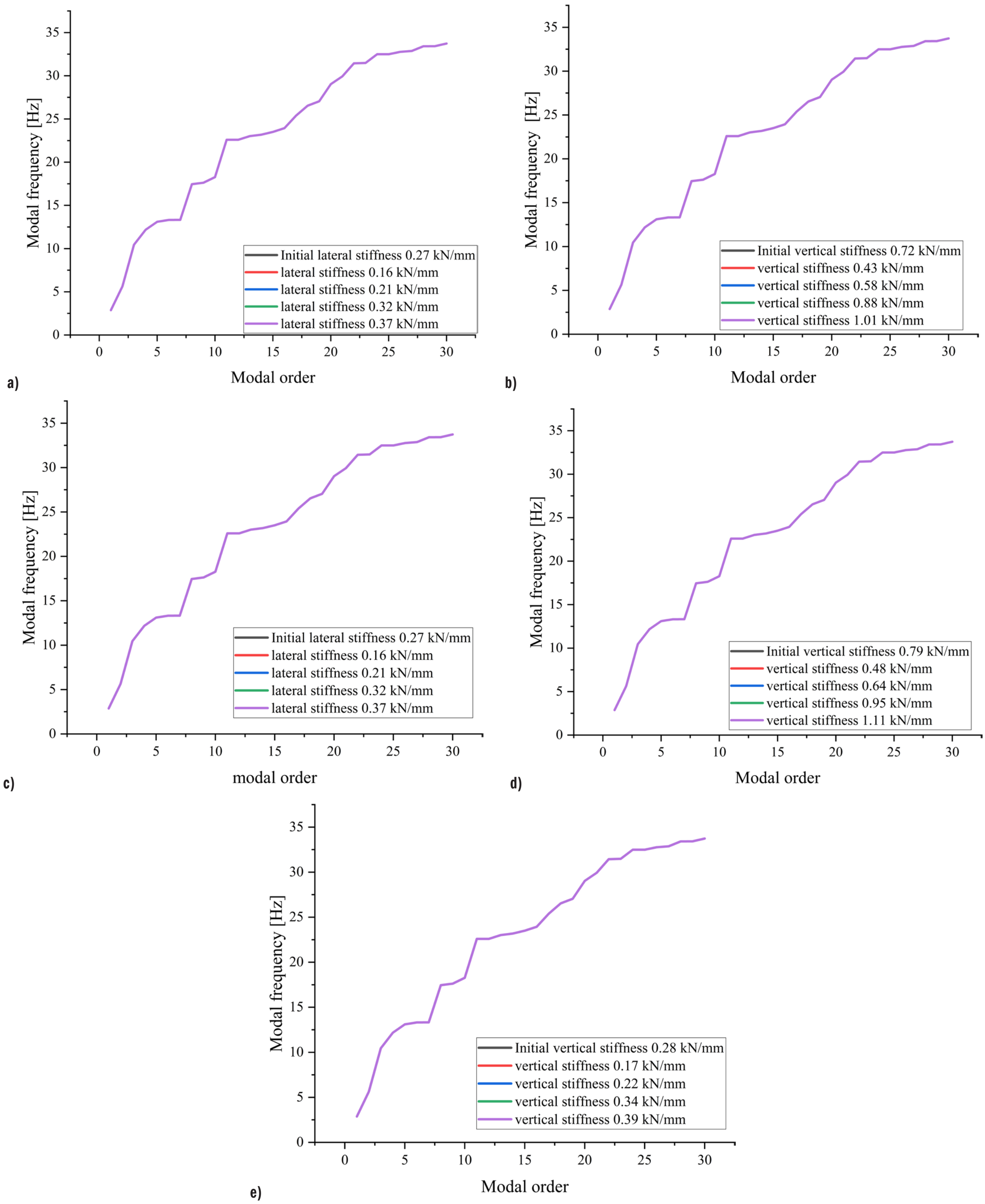

Fig. 4. Comparison with initial stiffness; a) transverse stiffness of the middle pillow spring, b) vertical stiffness of the middle pillow spring, c) transverse stiffness of the hinge spring, d) vertical stiffness of hinge springs, and e) vertical stiffness of damping springs

3.2 Effect of Bi-Series Transverse and Vertical Stiffness on Modal Frequency

To analyze the influence of the lateral and vertical stiffness of the spring and hinge, as well as the vertical stiffness of the damping spring, on the system's modal characteristics, a parametric study was conducted based on the C80 finite element model. In the baseline model, the lateral and vertical stiffness of the spring and hinge set to 0.27 kN/mm and 0.72 kN/mm, respectively, while the vertical stiffness of the damping spring was set to 0.28 kN/mm. For the sensitivity analysis, the lateral stiffness of the spring and hinge was varied at 0.16 kN/mm, 0.21 kN/mm, 0.32 kN/mm, and 0.37 kN/mm, while the vertical stiffness was set to 0.43 kN/mm, 0.58 kN/mm, 0.87 kN/mm, and 1.01 kN/mm. Additionally, the vertical stiffness of the damping spring was modified to 0.17 kN/mm, 0.22 kN/mm, 0.34 kN/mm, and 0.39 kN/mm. Through calculation, the modal frequencies and shapes of the first 30 modes were obtained, and the comparative results are shown in Fig. 4.

As shown in Fig. 4, the modal frequencies corresponding to different transverse and vertical stiffness values of the pillow spring, hinge spring, and damping spring were compared with those obtained under the initial stiffness parameters. The results indicate that, across all tested stiffness variations, the modal frequency changes remain below 1 %. This demonstrates that the lateral stiffness of the intermediate spring and hinge spring have a negligible influence on the system's modal frequency.

3.3 The Influence of Typical Mode Shapes on the Dynamic Performance of the Car Body

Through the measured excitation load of line loading as shown in Fig. 2c, the basic parameters of the railway wagon dynamic model were defined as follows: the car body load is 80 t, and the running speed is 70 km/h. For the first-series suspension, the stiffness values in the X, Y and Z directions are 3250 kN/m, 1500 kN/m, 8750 kN/m, respectively, while the corresponding damping values are 3250 Ns/m, 1500 Ns/m and 8750 Ns/m. For the second-series suspension, the stiffness values in the X, Y and Z directions are set to 0 kN/m, 0 kN/m, 460.45 kN/m and with all damping components set to 0 Ns/m. The rigid-flexible coupling dynamic model is solved using the Dell T7920 workstation with 10-core CPU parallel computation. Based on this configuration, the dynamic performance indices of the fully flexible C80 railway wagon, including derailment coefficient, wheel weight reduction rate, axle transverse force, and overturning coefficient, are obtained through dynamic simulation.

3.3.1 Effect of a Single Mode Shape on Dynamics

To quantify the influence of the typical mode shape of the car body on the dynamic performance of the railway wagon, the fully dynamic mode was used to analyze the influence of the primary modal for bending, torsion, and respiration. The dynamic performance index after the inhibition was compared with the initial dynamic performance index. The influence of different typical mode shapes on dynamic performance was then obtained. The comparison results are shown in Fig. 5.

As shown in Fig. 5a, suppressing different mode shapes has only a minimal effect on the derailment coefficient, and in all cases, the resulting values remain slightly lower than those in the initial (unsuppressed) state. In contrast, the effects of mode-shape suppression on the wheel load reduction rate varies significantly. Inhibition of the transverse bending and respiration mode shapes results in changes less than 1 %. However, the inhibition of torsional mode shapes leads to a pronounced increase, rising by 9.8 % to a value of 0.26 compared with the initial state. This finding highlights that torsional mode shapes play a dominant role in governing wheel load reduction rate behavior.

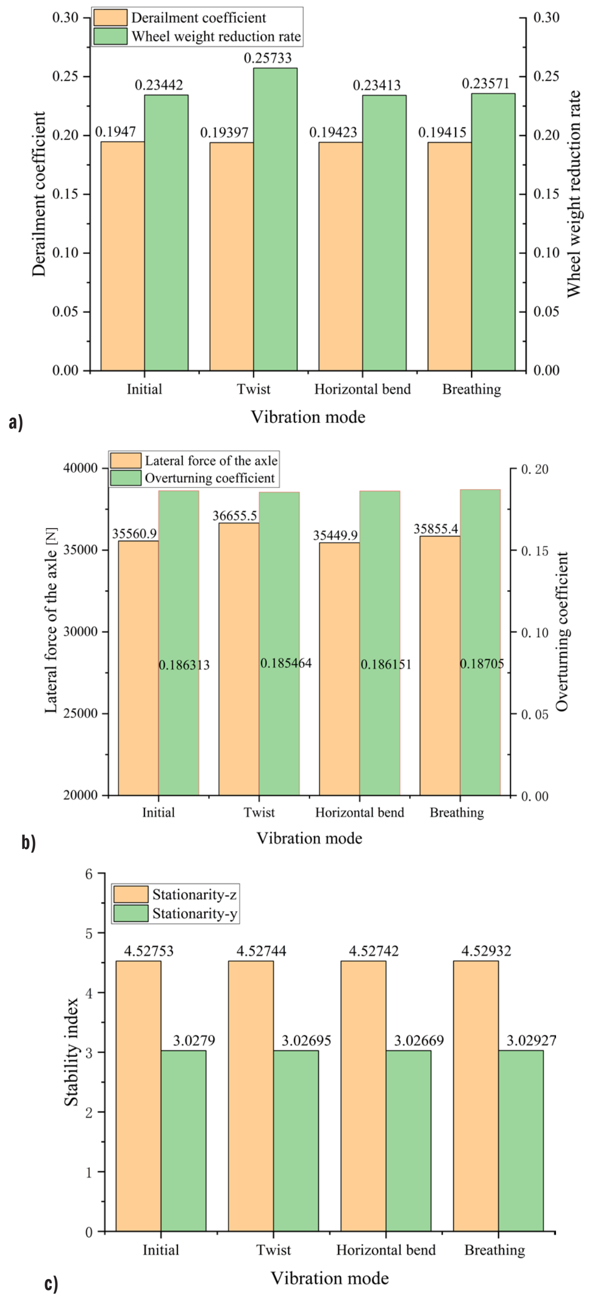

Fig. 5. Comparison of the dynamic performance of railway wagons; a) derailment coefficient and wheel weight reduction rate, b) axle transverse force and overturning coefficient, and c) stationarity index

For Fig. 5b, different mode shapes have a significant effect on the transverse force of the axle. When the torsional mode shape is inhibited, the transverse force increases sharply to 36.66 kN (peak value) when the torsional mode representing an increase of approximately 3 % compared with the initial conditions. In contrast, the transverse force of the inhibition transverse mode shape decreases to 35.45 kN, the lowest value among the four mode shapes and about 0.3 % below the initial value. Suppression of the breathing mode causes a slight increase to 35.86 kN, which remains about 2.2 % lower than the torsional mode shape. The appearance of its typical mode shapes helps to reduce the transverse force of the axle, providing an important reference for improving the vibration control strategies of railway wagons. For the overturning coefficient, suppressing the various mode shapes results in only marginal influence compared with the initial one. For Fig. 5c, the variation of the lateral and vertical stationarity indexes of the railway wagon relative to the initial state is below 0.1 % for all three mode-shape suppression scenarios (torsional, transverse bending, and respiratory mode shapes). This indicates that the torsional, transverse bending, and breathing mode shapes on the stationarity of railway wagons exert only a minimal influence of heavy trains during the operation.

Table 1. **Dynamical indicators of typical mode shapes affect the weights**

Serial number	Dynamic index	Typical vibration mode [%]		
		Twist	Horizontal bend	Breathing
1	Derailment coefficient	41.83	31.32	26.85
2	Wheel weight reduction rate	93.58	1.15	5.27
3	Lateral force of the axle	72.97	7.4	19.63
4	Overturning coefficient	48.57	9.27	42.16
5	Stationarity-y	27.46	34.97	37.57
6	Stationarity-z	4.52	5.53	89.95

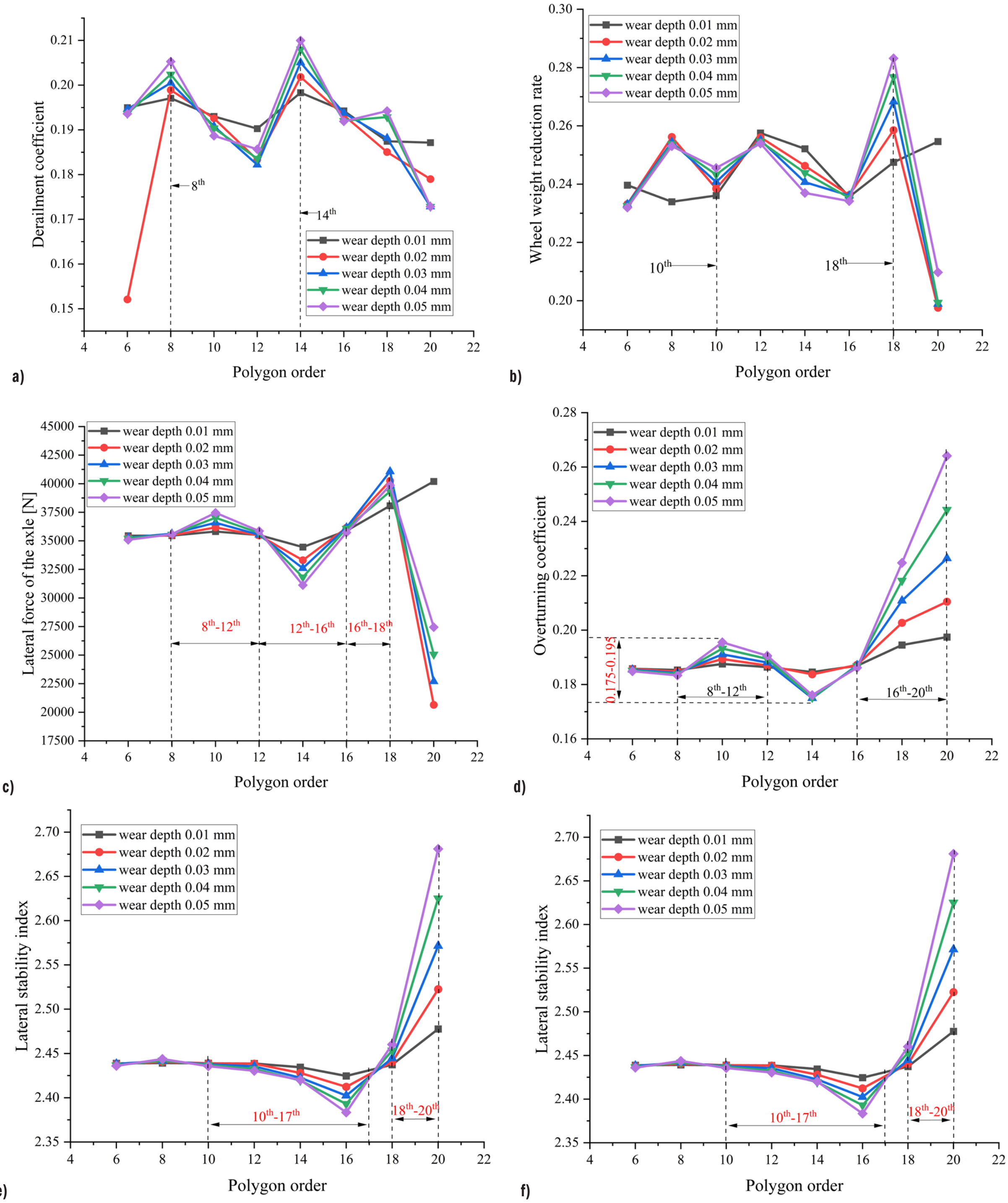

Fig. 6. **Dynamic performance of railway wagons at different depths; a) derailment coefficient, b) wheel weight reduction rate, c) lateral force of the axle, d) overturning coefficient, e) lateral stability index, and f) vertical stability index**

3.3.2 Typical Mode Shape Weighting Effects

To analyze the influence of the typical mode shapes of the C80 car body on the dynamic performance indexes, the torsional, lateral bending and respiration mode shapes were individually suppressed. The resulting variation rates of each dynamic performance index relative to the initial dynamic indicators were obtained. By normalizing these variation rates, the corresponding influence weights of three typical mode shapes under each dynamic metric were obtained, as shown in Table 1.

It is shown in Table 1, that the torsional mode shape exhibits the highest influence weights on the derailment coefficient, wheel weight reduction rate, axle transverse force and overturning coefficient, with corresponding values of 41.83 %, 93.58 %, 72.97 %, and 48.57 %, respectively. The lateral and vertical stationarity indexes are dominated by the respiratory mode shape, reaching 37.57 % and 89.95 %, respectively. Therefore, their influence must be carefully considered in structural design and suspension parameter optimization.

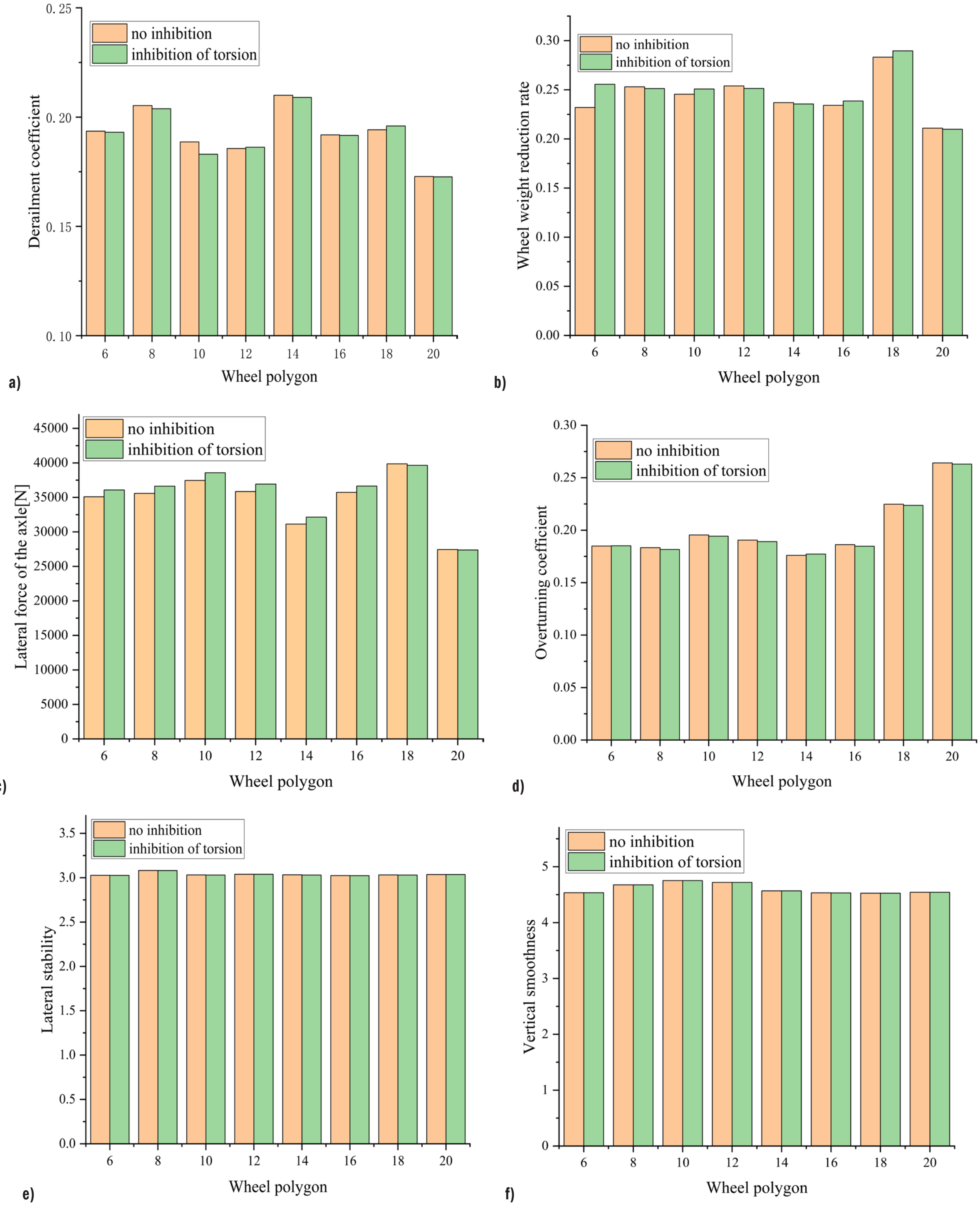

Fig. 7. Comparison of the dynamic performance of railway wagons with or without suppressed torsional mode shapes; a) derailment coefficient, b) wheel weight reduction rate, c) lateral force of the axle, d) overturning coefficient, e) lateral stability, and f) vertical smoothness

3.4 Effect of Wheel Polygons and Typical Mode Shapes on Dynamic Performance

3.4.1 Influence of Wheel Polygons

Based on the fully flexible dynamic model of the railway wagon, the dynamic performance of the heavy vehicle operating at a speed of 70 km/h on the straight track was studied. The 6th, 8th, 10th, 12th, 14th, 16th, 18th, and 20th order wheel polygons were introduced, with corresponding wear depths of 0.01 mm, 0.02 mm, 0.03 mm, 0.04 mm, and 0.05 mm. The simulation results for all condition are shown in Fig. 6.

As shown in Fig. 6a, when the vehicle speed and the polygon order remain constant, the derailment coefficient increases with increasing polygon wear depth under the 8th and 14th order conditions. These two polygon orders exert a more pronounced destabilizing effect on the derailment coefficient during the operation of heavy-haul railway, therefore, special attention should be given. For Fig. 6b, at the constant vehicle speed and wheel polygon order, the wheel weight reduction rate increases as the polygon wear depth grows, particularly under the 10th and 18th order conditions. The increase is especially significant for the 18th order condition, where the wear depth of 0.05 mm is 14.4 % higher compared with the wear depth of 0.01 mm. This finding highlights the necessity of controlling the wear depth to mitigate wheel load reduction rate.

For Fig. 6c, when the speed and the polygon order remain constant, the axle transverse force increases with the polygon wear depth at orders 8th to 12th and 16th to 18th. In contrast, the axle transverse force decreases as the polygon wear depth increases within the 12th to 16th order range, indicating that the axle transverse force is inhibited by the wear depth at the 12th to 16th order. As shown in Fig. 6d, when the vehicle speed and the wheel polygon order are constant, the overturning coefficient increases with the increase of the polygon wear depth for the 8th to 12th and 16th to 20th orders. This effect is especially pronounced for higher-order polygons: under the 20th order condition, the overturning coefficient at a wear depth 0.05 mm is 33.76 % higher than that at 0.01 mm. To ensure the operation safety of railway wagons, it is necessary to impose safety limits on the polygon abrasion depth under different working conditions.

From Fig. 6e, when the vehicle speed and polygon order remain constant, the lateral stationarity index decreases with increasing polygon wear depth for the 10th to 17th orders. In contrast, for the 18th to 20th polygon orders, the lateral stationarity index increases as the wear depth increases. This indicates that wear depth inhibits lateral stationarity index in the 10th to 17th orders, whereas for higher-order polygons (18th to 20th) excessive wear depth leads to a rapid deterioration of lateral stationarity. For Fig. 6f, when the vehicle speed and polygon order remain constant, the vertical (sag) stationarity index decreases with increasing polygon wear depth for the 9th to 16th order conditions. This trends indicate that the lateral stationarity index is relatively insensitive to wear depth within 9th to 16th order conditions.

3.4.2 Effect of Torsional Mode Shapes on Dynamic Performance

To analyze the dynamic performance under torsional mode-shape conditions, the influence of inhibiting and not inhibiting torsional mode shape were evaluated using the fully flexible railway wagon dynamic model. Wheel polygons of 6th, 8th, 10th, 12th, 14th, 16th, 18th and 20th orders were set, with a fixed wear depth of 0.05 mm and the running speed of 70 km/h. The resulting dynamic performance indices under both conditions were compared, and the comparison results are presented in Fig. 7.

As shown in Fig. 7a, the derailment coefficient remains below the safety limit of 1.0 regardless of whether the torsional mode shape is suppressed. In addition, the maximum variation increases by 3 % under the 10th order condition compared with the non-inhibition condition. This indicate that although the torsional mode shape does influence the derailment coefficient of the railway wagon, its overall effect remains limited. For Fig. 7b, the behavior of the wheel load reduction rate is strongly dependent on the relationship between the wheel polygon order and the torsional mode frequencies. At the 8th, 12th, 14th and 20th order polygon conditions, the characteristic frequencies are close to the torsional vibration mode frequencies. This suppresses the torsional vibration condition of the vehicle. Compared to the situation without suppression, the wheel load reduction rate decreases. Therefore, based on the wheel polygon, choosing to suppress the torsional vibration can reduce the wheel load reduction rate. After suppressing the torsional vibration at the 6th, 10th, 16th and 18th order, the vibration balance is disrupted. Compared to the situation without suppression, the wheel load reduction rate increases relative to the unsuppressed case. Especially in the 6th order condition, where suppression causes the wheel load reduction rate to rise by 9.85 %, indicating the significant impact of the wheel load reduction rate.

For Fig. 7c, except for the 18th and 20th order polygon conditions, the axle transverse force under torsional-mode suppression is greater than that without inhibition. Especially, under the 14th order condition, the transverse force increases by 3.3 %, indicating that the torsional mode shape has a measurable influence on the axle transverse force of railway wagons. As shown in Fig. 7d, except for the 6th and 14th order working conditions, the overturning coefficient of the inhibited torsional mode shape generally decreases. This indicates that torsional mode shape can effectively reduce the overturning coefficient of railway wagons. From Figs. 7e and the variations in both the lateral and vertical stationarity indexes remain below 1 % under the condition of inhibiting torsional mode shapes. This indicates that the torsional mode shapes exert only a minimal influence on the transverse and vertical stationarity indicators.

4 CONCLUSION

1. A modal finite element simulation model was established based on the C80 railway freight car. Both the vehicle-level modal frequency and the system-level modal frequency increase as the first series lateral and vertical stiffness increase. Across all conditions, the system-level modal frequency remains lower than the corresponding vehicle-level modal frequency.
2. When vehicle speed and wheel polygon order are fixed, in the 8th to 12th and 16th to 20th order working conditions, the overturning coefficient increases with the polygonal wear depth. Notably, the 0.05 mm abrasion depth in the 20th order working condition increases by 33.76% compared with the 0.01 mm abrasion depth. This demonstrates that the wheel polygon wear depth has a pronounced effect on overturning stability.
3. Suppressing torsional vibration mode for 8th, 12th, 14th and 20th wheel polygons reduces the wheel load reduction rate by 1 % compared with the unsuppressed case. This suggests that targeted torsional-mode control can improve wheel–rail load distribution for specific polygon orders. However, under the 6th order, 10th order, 16th order and 18th orders suppressing torsional mode increases the wheel weight reduction rate compared with that without inhibition, especially under the 6th order condition, where the wheel weight reduction rate increases by 9.85 %. This indicates that torsional mode shape can also deteriorate wheel weight reduction rate performance of railway wagons.

Collectively, the study on the dynamic performance of C80 railway freight cars under the influence of wheel polygon shapes and typical body vibration modes provides important engineering guidance highlighting the coupled influence of wheel polygonal wear and typical car-body vibration modes on derailment safety, wheel unloading behavior, and overall running stability.

References

[1] Nielsen, J.C.O., Johansson, A. Out-of-round railway wheels-a literature survey. *Proc Inst Mech Eng F-J Rail Rapid Transit* 214 79-91 (2000) **DOI:10.1243/0954409001531351**.

[2] Zhang, F., Wu, P., Wu, X., He, X., Zhang, M. et al. Analysis of the influence of polygons on axle boxes of high-speed train wheels. *J Vibr Measur Diagn* 38 1063-1068 (2018) **DOI:10.16450/j.cnki.issn.1004-6801.2018.05.029**. (in Chinese)

[3] Li, H., Li, L., Zhang, Y., Ye, C., Sun, Y., Yu, X., et al. Research on the influence of wheel profile wear coupled with wheel polygon on the dynamic response of vehicles. *J Railway Sci Eng* 21 4240-4252 (2024) **DOI:10.19713/j.cnki.43-1423/u.T20232081**. (in Chinese)

[4] Tao, G., Wen, Z., Liang, X., Ren, D., Jin, X. An investigation into the mechanism of the out-of-round wheels of metro train and its mitigation measures. *Vehic SystDynam* 57 1-16 (2019) **DOI:10.1080/00423114.2018.1445269**.

[5] Cai, W., Chi, M., Tao, G., Wu, G., Wu, X., Wen, Z. Experimental and numerical investigation into formation of metro wheel polygonalization. *Shock Vibr* 2019 1538273 (2019) **DOI:10.1155/2019/1538273**.

[6] Yang, Y., Chai, F., Liu, P., Ling, L., Wang, K., Zhai, W. On the polygonal wear evolution of heavy-haul locomotive wheels due to wheel/rail flexibility and its mitigation measures. *Chin J Mech Eng* 37 16 (2024) **DOI:10.1186/s10033-024-01001-z**.

[7] Jin, X., Wu, Y., Liang, S., Wen, Z., Wu, X., Wang, P. Characteristics, mechanism, influences and countermeasures of polygonal wear of high-speed train wheels. *J Mech Eng* 56 118-136 (2020) **DOI:10.3901/JME.2020.16.118**. (in Chinese)

[8] Zhou, Z., Liu, Y., Guo, T., Wang, T., Huo, W. Study on the mechanism of polygonal wear in wheels based on wheel-rail contact normal force. *Int Conf Artif Intell Autonom Transp. Springer Nature* 458-465 (2024) **DOI:10.1007/978-981-96-3969-4_49**.

[9] Johansson, A., Nielsen, J. Out-of-round railway wheels-wheel-rail contact forces and track response derived from field tests and numerical simulations. *Proc Inst Mech Eng F-J Rail Rapid Transit* 217 135-146 (2003) **DOI:10.1243/095440903765762878**.

[10] Johansson, A., Andersson, C. Out-of-round railway wheels-a study of wheel polygonalization through simulation of three-dimensional wheel-rail interaction and wear. *Vehic Syst Dynam* 43 539-559 (2005) **DOI:10.1080/00423110500184649**.

[11] Ye, Y., Qu, S., Wei, L., Li, D., Huang, C., Wang, J. et al. Localized rail third-order bending mode causes high-order polygonization of high-speed train wheels. *Mech Syst Signal Proces* 223 111816 (2025) **DOI:10.1016/j.ymssp.2024.111816**.

[12] Yang, X., Tao, G., Li, W., Wen, Z. On the formation mechanism of high-order polygonal wear of metro train wheels: Experiment and simulation. *Eng Failure Analys* 127 105512 (2021) **DOI:10.1016/j.engfailanal.2021.105512**.

[13] Wu, Y., Du, X., Zhang, H., Wen, Z., Jin, X. Experimental analysis of the mechanism of high-order polygonal wear of wheels of a high-speed train. *J Zhejiang Univ-Scie A* 18 579-592 (2017) **DOI:10.1631/jzus.A1600741**.

[14] Fu, D., Wang, W., Dong, L. Analysis on the fatigue cracks in the bogie frame. *Eng Fail Anal* 58 307-319 (2015) **DOI:10.1016/j.engfailanal.2015.09.004**.

[15] Wang, B., Xie, S., Jiang, C., Along, Q., Sun, S., Wang, X. An investigation into the fatigue failure of metro vehicle bogie frame. *Eng Fail Anal* 118 104922 (2020) **DOI:10.1016/j.engfailanal.2020.104922**.

[16] Liu, X., Zhai, W. Analysis of vertical dynamic wheel/rail interaction caused by polygonal wheels on high-speed trains. *Wear* 314 282-290 (2014) **DOI:10.1016/j.wear.2013.11.048**.

[17] Song, Y., Zhang, X., Sun, B. Influence of polygonal wear on dynamic performance of wheels on high-speed trains. *Tehn Vjest* 28 27-33 (2021) **DOI:10.17559/TV-20190103105240**.

[18] Wu, X., Rakheja, S., Qu, S., Wu, P., Zeng, J., Ahmed, A.K.W. Dynamic responses of a high-speed railway car due to wheel polygonalisation. *Vehic Syst Dyn* 56 1817-1837 (2018) **DOI:10.1080/00423114.2018.1439589**.

[19] Barke, D.W., Chiu, W.K. A review of the effects of out-of-round wheels on track and vehicle components. *Proc Inst Mech Eng F-J Rail Rapid Trans* 219 151-175 (2005) **DOI:10.1243/095440905X8853**.

[20] Zhang, J., Han, G., Xiao, X., Wang, R., Zhao, Y., Jin, X. Influence of wheel polygonal wear on interior noise of high-speed trains. *Chi High-Speed Rail Tech* 373-401 (2018) **DOI:10.1007/978-981-10-5610-9_20**.

[21] Thomas, D., Berg, M., Stichel, S. Measurements and simulations of rail vehicle dynamics with respect to overturning risk. *Vehic Syst Dyn* 48 97-112 (2010) **DOI:10.1080/00423110903243216**.

[22] Park, J.H., Koh, H.I., Kim, N.P. Parametric study of lateral stability for a railway vehicle. *J Mech Sci Tech* 25 1657-1666 (2011) **DOI:10.1007/s12206-011-0421-0**.

[23] Ma, S., Wang, H., Yao, Y., Ding, W. Stability analysis of high-speed vehicles considering the non-diagonal stiffness of a series of steel springs and frame flexibility. *Mech Des Manuf* 6 300-304 (2023) **DOI:10.19356/j.cnki.1001-3997.20230307.005**. (in Chinese)

[24] Guan, Q., Wen, Z., Chi, M., Liang, S. Phase synchronization modal analysis of wheelset hunting motion. *J Mech Eng* 57 279-288 (2021) **DOI:10.3901/JME.2021.24.279**. (in Chinese)

[25] Xiao, Q., Cheng, Y., Luo, J., Zhou, S., Zhou, Q., Cao, T. Sensitivity analysis of high-speed train wheel vibration influenced by vehicle-track coupling. *J Traff Transp Eng* 21 160-169 (2021) **DOI:10.19818/j.cnki.1671-1637.2021.06.012**. (in Chinese)

[26] Lei, X., Wang, Z., Luo, K. Research on the dynamic performance of Nanchang metro vehicles. *J Rail Sci Eng* 14 2460-2466 (2017) **DOI:10.19713/j.cnki.43-1423/u.2017.11.025**.

[27] Mousavi Bideleh, S.M., Berbyuk, V. Global sensitivity analysis of bogie dynamics with respect to suspension components. *Multibody Syst Dyn* 37 145-174 (2016) **DOI:10.1007/s11044-015-9497-0**.

[28] Cascino, A., Meli, E., Rindi, A. A new strategy for railway bogie frame designing combining structural-topological optimization and sensitivity analysis. *Vehicles* 6 651-665 (2024) **DOI:10.3390/vehicles6020030**.

[29] Cascino, A., Meli, E., Rindi, A. . Development of a design procedure combining topological optimization and a multibody environment: Application to a tram motor bogie frame. *Vehicles* 6 1843-1856 (2024) **DOI:10.3390/vehicles6040089**.

[30] Luo, R.K., Gabbitas, B.L., Brickle, B.V. Fatigue life evaluation of a railway vehicle bogie using an integrated dynamic simulation. *Proc Inst Mech Eng F-J Rail Rapid Transit* 208 123-132 (1994) **DOI:10.1243/PIME_PROC_1994_208_242_02**.

[31] Luo, R.K., Gabbitas, B.L., Brickle, B.V. Dynamic stress analysis of an open-shaped railway bogie frame. *Eng Fail Anal* 3 53-64 (1996) **DOI:10.1016/1350-6307(95)00030-5**.

[32] Cascino, A., Meli, E., Rindi, A. Dynamic size optimization approach to support railway carbody lightweight design process. *Proc Inst Mech Eng F-J Rail Rapid Transit* 237 871-881 (2022) **DOI:10.1177/0954409722114093**.

[33] Tang, J., Zhou, Z., Chen, H., Wang, S., Gutiérrez, A. Research on the lightweight design of GFRP fabric pultrusion panels for railway vehicle. *Compos Struct* 286 115221 (2022) **DOI:10.1016/j.compstruct.2022.115221**.

[34] Cascino, A., Meli, E., Rindi, A. Comparative analysis and dynamic size optimization of aluminum and carbon fiber thin-walled structures of a railway vehicle car body. *Materials* 18 1501 (2025) **DOI:10.3390/ma18071501**.

[35] Cascino, A., Meli, E., Rindi, A. A strategy for lightweight designing of a railway vehicle car body including composite material and dynamic structural optimization. *Rail Eng Sci* 31 340-360 (2023) **DOI:10.1007/s40534-023-00312-6**.

[36] Zhou, L., Wang, G., Sun, K., Li, X. Trajectory tracking study of track vehicles based on model predictive control. *Stroj Vest-J Mech E* 65 329-342 (2019) **DOI:10.5545/sv-jme.2019.5980**.

[37] Yu, Y., Song, Y., Zhao, L., Zhou, C. Analytical formulae and applications of vertical dynamic responses for railway vehicles. *Stroj Vest-J Mech E* 69 73-81 (2023) **DOI:10.5545/sv-jme.2022.375**.

Acknowledgement *The authors would like to thank for the support for ties work by Research Program supported by General Program of Henan Provincial Natural Science Foundation (Project No.: 252300421908), China, Open Project of the State Key Laboratory of Rail Transit Vehicle System (RVL2509), China and by Heilongjiang Provincial Postdoctoral Science Project (grant numbers LBH-Z23041), China.*

Received: 2025-07-10, revised: 2025-09-24, 2025-10-22, accepted: 2025-10-29 *as Original Scientific Paper.*

Declaration of Conflicting Interests *The author(s) declared no potential conflicts of interest with respect to the research, authorship, and/or publication of this article.*

Data Availability *The data that supports the findings of this study are available from the corresponding author upon reasonable request.*

Author Contribution *Yuru Li: Conceptualization, Methodology, Formal analysis, Investigation, Visualization, Writing—original draft; Gangjian Zhou: Formal analysis, Investigation, Visualization, Writing—review and editing; Xiangwei Li: Formal analysis, Investigation; Tao Zhu: Formal analysis, Investigation; Shangchao Zhao: Formal analysis, Investigation; Chunlei Zhao: Formal analysis, Investigation; Junke Xie: Conceptualization, Formal analysis, Investigation; Shoune Xiao: Conceptualization, Formal analysis, Investigation, Supervision.*

Dinamično obnašanje železniškega vagona C80 pod vplivom poligonalnosti koles in značilnih oblik nihanja karoserije

Povzetek *Za raziskavo vpliva značilnih oblik nihanja in poligonalnosti koles na dinamične lastnosti karoserije železniškega tovornega vagona je bil v tej raziskavi izbran vagon C80. Razvita sta bila model na ravni vozila in model na ravni sistema z metodo končnih elementov, ki sta pokazala, da bočna in navpična togost tovornih vagonov pomembno vplivata na sistemske lastne oblike. Nadalje je bila z uporabo so-simulacije med programoma NASTRAN in SIMPACK vzpostavljena popolnoma fleksibilna dinamična simulacija vagona C80. Analiziran je bil vpliv značilnih lastnih frekvenc na dinamično obnašanje vagona ob upoštevanju poligonalnosti koles in parametrov obrabe. Rezultati kažejo, da omejitev torzijske oblike nihanja vagona zmanjša njen vpliv na koeficient iztirjenja, stopnjo zmanjšanja obremenitve koles, prečno silo osi in koeficient prevračanja za več kot 40 %. Ko se hitrost vlaka ujema z redom poligonalnosti koles, se stopnja zmanjšanja obremenitve koles povečuje z globino obrabe pri poligonalnosti 10. in 18. reda. Pri slednjem se ob povečanju globine obrabe z 0,01 mm na 0,05 mm poveča za kar 14,4 %. Poleg tega je bilo ugotovljeno, da omejitev torzijske oblike bistveno poveča stopnjo zmanjšanja obremenitve koles pri poligonalnosti 6., 10., 16. in 18. reda, zlasti pri poligonalnosti 6. reda. Raziskava nudi smernice za optimizacijo parametrov vzmetenja in nadzor poligonalne obrabe koles pri železniških vagonih ter predstavlja teoretično osnovo za izboljšanje njihove dinamične zmogljivosti.*

Ključne besede *popolna fleksibilnost, železniški vagon C80, dinamični modeli, poligonalnost koles, parametri vzmetenja*